HHS Public Access

Author manuscript

Magn Reson Med. Author manuscript; available in PMC 2015 May 13.

Published in final edited form as:

Magn Reson Med. 2014 February ; 71(2): 570–579. doi:10.1002/mrm.24692.

Renal Perfusion Imaging with Two-Dimensional Navigator Gated Arterial Spin Labeling

Huan Tan[1], **Ioannis Koktzoglou**[1,2], and **Pottumarthi V. Prasad**[1,2]

[1]Department of Radiology, NorthShore University HealthSystem, Evanston, Illinois, USA

[2]The University of Chicago Pritzker School of Medicine, Chicago, Illinois, USA

Abstract

Purpose—To develop a navigator technique enabling free-breathing acquisition to afford sufficient signal averaging for quantitative renal perfusion measurement using arterial spins labeling (ASL) MRI.

Methods—A novel two-dimensional (2D) navigator technique was implemented in concert with FAIR (flow-sensitive alternating inversion recovery) preparation and True-FISP (true fast imaging with steady possession) readout. The navigator images were obtained with a low resolution FLASH (fast low angle shot) readout at end of each ASL acquisition. A retrospective algorithm was developed to automatically detect respiratory motion for selective signal averaging. The 2D navigator-gated FAIR True-FISP was performed in ten healthy volunteers and five patients with chronic kidney disease (CKD).

Results—Excellent image quality and comparable cortical perfusion rates (healthy: 276 ± 28 ml/100g/min, patients: 155 ± 25 ml/100g/min) to literature values were obtained. An average of three-fold SNR improvement was obtained in the 2D navigator-gated approach compared to the breath-hold acquisition in the healthy volunteers. Good image quality was achieved in patients while the results from breath-hold acquisition were unusable. The quantitative perfusion rates were significantly lower in CKD patients compared to the healthy volunteers.

Conclusion—2D navigator-gated free breathing ASL is feasible and offers a non-invasive method to evaluate renal perfusion both in healthy subjects and those with CKD.

Keywords

2D Navigator; Renal Perfusion; FAIR True-FISP; Respiratory Motion

INTRODUCTION

Quantitative change in tissue perfusion can provide valuable information regarding organ function in different pathological conditions. Kidney is a highly perfused organ, and renal perfusion measurement can directly indicate functional impairments including inflammatory and degenerative renal disease, renal artery stenosis, renal transplant nephropathy, chronic

Corresponding Author: Huan Tan, Department of Radiology, NorthShore University HealthSystem, 2650 Ridge Ave., Evanston, IL 60201, htan@northshore.org, Phone: 847-570-4807, Fax: 847-570-2942.

ischemic nephropathy and drug induced nephropathy (1). The use of contrast agents has been pursued to evaluate first pass perfusion MRI and glomerular filtration rate measurements (1). However, given the risk of nephrogenic systemic fibrosis (2,3), the use of gadolinium-based contrast agents is contraindicated in patients with compromised renal function.

Arterial spin labeling (ASL) is a non-invasive technique that uses water in the blood as an endogenous tracer to measure perfusion (4). The principle of ASL involves acquiring two images: a label image where spins in the inflow blood have been magnetically tagged (usually by inversion), and a control image where the magnetization of the inflowing spins is unaltered. By subtracting the label from the control image, the static tissue signal cancels out and the difference signal is then proportional to the local tissue perfusion. One drawback of the ASL technique is its intrinsically low signal-to-noise ratio (SNR) owing to the limited fractional blood volume in most tissues. Healthy kidneys have sufficiently high fractional blood volume and hence quantitative ASL has been shown to be feasible. However, in pathological cases, signal averaging is usually required in order to obtain adequate image quality. Since its initial introduction nearly two decades ago, ASL has been well established and applied extensively for brain studies (5). The number of studies applying ASL in the kidneys has also been steadily increasing (6-9), however mostly in healthy subjects.

As a subtraction based technique, ASL is inherently prone to motion induced errors and artifacts. A mismatch between control and label image can result in artifacts and inaccurate perfusion estimation. The major challenge in performing ASL in the kidneys is the abdominal motion caused by respiration. While in-plane motion may be corrected via post-processing, it is difficult to retrospectively correct for through-plane motion. Several acquisition strategies have been proposed to solve this problem, including single / multiple breath-holds, synchronized breathing, and respiratory triggering (9,10). However, those strategies are still prone to residual motion and impractical for routine clinical use. In particular, breath-holding can be difficult to tolerate for patients. Current state of the free-breathing acquisition requires significant amount of manual post-processing, and is impractical for routine clinical implementation.

In this study, we implemented a novel 2D navigator with FAIR (flow-sensitive alternating inversion recovery) True-FISP (true fast imaging with steady precession) sequence (8,11) to measure renal perfusion in a free-breathing acquisition. An automated post-processing algorithm was developed to estimate the diaphragm position on the 2D navigator images as a reference to select the final control and label images for perfusion calculation. The purpose of this study was to minimize respiration-induced kidney motion via selective signal averaging according to the navigator data. The preliminary results were obtained in healthy volunteers and a small number of patients with chronic kidney diseases (CKD). The SNR and perfusion quantification results from free-breathing acquisitions were compared to the breath-hold acquisitions.

METHODS

Pulse Sequence Design

The renal perfusion measurement was performed using the FAIR True-FISP sequence (8). The pulse sequence diagram is illustrated in Figure 1. Details of each pulse sequence component are described as follows.

2D FLASH Navigator—The 2D navigator was employed immediately after the True-FISP acquisition. The aim was to acquire a low resolution 2D image to estimate respiratory motion based on the diaphragm position throughout the respiration cycle. The final perfusion weighted image was computed by only using control and label images considered to be at the same diaphragmatic position. We assumed there was no significant motion during the True-FISP and the navigator readout. The 2D navigator comprised a 2D FLASH (fast low angle shot) sequence with the following parameters: flip angle = 5°, TR/TE = 2.2/1.2 ms, field of view = 400 mm, image matrix size = 96 × 96, receiver bandwidth = 1000 Hz/Pixel, 5/8 partial Fourier encoding along the phase encoding direction, parallel acceleration = 2 with 10 integrated reference lines for calibrating coil sensitivities. The navigator was prescribed graphically to cover the right hemidiaphragm in either sagittal or coronal plane. The total duration for the 2D navigator was 75 ms.

FAIR True-FISP Sequence—In FAIR, perfusion weighting was achieved by a pair of slice selective (control) and global inversion (label) pulses employed in an interleaved manner (11). A 10.24 ms adiabatic FOCI pulse (μ= 6, β=1078) was used for inversions (12). The slice selective inversion band was positioned carefully to avoid intersection with major arteries. The inversion slab thickness was set to 30 mm to accommodate expected through-plane motion (8,13). True-FISP imaging was performed after the inversion pulse following a brief delay (TI) to allow tagged blood to perfuse into the tissue. A TI of 1.5 sec was used for healthy volunteers. A TI of 2 sec was used for patients in consideration of potentially comprised flow. The imaging slice was positioned in an oblique coronal orientation to match the longitudinal axis of both kidneys. The following imaging parameters were used: flip angle = 60°, echo spacing / TE = 4 / 2.02 ms, TR = 3 sec, receiver bandwidth = 651 Hz/Pixel, image matrix = 128 × 128, field of view = 360 – 400 mm, imaging slice thickness = 8 mm. To minimize artifacts from the oscillatory transient effects in the True-FISP acquisition, a ramp of 10 RF pulses with linearly increasing flip angles was employed at the beginning of the acquisition without signal recording (14). Centric ordered phase encoding was used to maximize perfusion sensitivity.

In-vivo Experiments

All experiments were performed on a 3T MRI system (MAGNETOM Verio, Siemens Healthcare, Erlangen, Germany) equipped with high performance gradient coils (45 mT/m maximum gradient strength, 200 mT/m/ms slew rate). The body coil was used as the transmitter, and the combination of spine and body array coils was used as the receiver. Subjects were positioned feet first and all imaging was performed at the magnet isocenter. Ten healthy volunteers (5 male, 5 female, 42 ± 16 years of age) and five patients with CKD (2 male and 3 female, 64 ± 12 year of age) were recruited with the approval from our

Institutional Review Board. Written informed consent was obtained from each participant prior to the study.

Healthy Volunteer Experiment 1—The purpose of this experiment was to test the feasibility of the 2D navigator technique. Eight subjects participated in this study. The volunteers were instructed to relax and breathe normally during the scans. FAIR True-FISP sequence was repeated with the 2D navigator positioned in the sagittal and coronal plane, respectively. 50 control/label pairs were with a total scan time of 5 minutes per free-breathing scan. An 18 sec breath-hold scan was performed at expiration with 3 control/label pairs. A proton density weighted (M_0) image was acquired using an identical True-FISP readout with a TR of 10 sec and no inversion pulses. In addition, a high resolution renal perfusion image (matrix size = 256 × 256, slice thickness = 5mm) was acquired in healthy volunteers. An iPAT acceleration factor of 2 was used in these high resolution scans to reduce readout duration.

Healthy Volunteer Experiment 2—The purpose of the experiment is to test the robustness of the navigator technique in the presence of different inversion band thicknesses, imaging planes and respiratory patterns. Three subjects participated in this study. A total of 12 perfusion scans were included in this experiment: three labeling inversion band thicknesses of 10, 20 and 30 mm were used; the imaging plane was prescribed in both transverse and oblique coronal plane; each scan was performed twice where the subject was instructed to breathe normally on one and deeply on the other. The remaining imaging parameters were identical to experiment 1. Due to the time constraint, the 2D navigator was prescribed only in the coronal plane.

Patient Experiment—FAIR True-FISP with the 2D navigator was tested in five patients with CKD stage 2 - 4. The imaging protocol was identical to what was used in healthy volunteer experiment 1, except for using a TI = 2 seconds. Two patients were scanned for 5 minutes and three patients were scanned for 10 minutes. A breath-hold scan was performed for comparison.

Data Processing

Raw perfusion and navigator data was transferred to a local workstation (Intel i7 2.7 GHz Quad Core, 8 Gigabytes of RAM) for the image reconstruction. Control and label images were reconstructed with the 2D inverse Fourier transform followed by the square root of the sum of the squares to combine the data from different coils. The navigator images and the high resolution FAIR True-FISP images were reconstructed using GRAPPA (Generalized Autocalibrating Partially Parallel Acquisition) (15) when parallel acceleration was employed. The first control/label pair in the temporal series for all perfusion scans was considered to be acquired before a stable longitudinal steady state was achieved, and was discarded from the subsequent calculation. All data reconstruction and image analysis were performed using MATLAB (MathWorks, Natick, MA).

Automated Retrospective Signal Averaging with the 2D Navigator—The kidneys were assumed to be in the same position on the 2D navigator image and its corresponding

control/label image. To minimize through-plane motion, an automated strategy for retrospective signal averaging was developed in the following steps:

1. Sub-navigator identification. The longitudinal kidney motions can be approximated by the diaphragmatic movement at the border of lung and liver. A rectangular subregion in the navigator images (referred to as the sub-navigator) along right hemidiaphragm would be an ideal location to detect the through-plane motion. To locate the sub-navigator automatically, the navigator images from the entire temporal series were first averaged into a single image. A general area where the right hemidiaphragm resides was estimated and extracted from the averaged navigator image. Given the center of the imaging plane was often positioned medially on the spine with one kidney on each side, the area containing the right hemidiaphragm was estimated as the top left quadrant in the coronal navigator image or the top middle half in the sagittal navigator image. The sub-navigator position was then identified by computing the normalized 2D cross-correlation (16) of the extracted diaphragm area and a predefined template. The template was defined as a 2 × 21 (row × column) matrix where values in columns 1 – 7 were set to 0, values in columns 8 – 14 were set to linearly increase from 0 to 1 with a slope of 0.14, and values columns 15 – 21 were set to 1. The purpose of the template was to mimic the signal intensity transition from the lung to the liver on the navigator images. The template matrix was determined empirically. The region with the peak correlation value was identified as the sub-navigator. An illustration of the 2D navigator images (Figure 2a) and the sub-navigator identification process is shown in Figure 2.

2. Diaphragmatic motion detection. A 2 × 21 (row × column) matrix was extracted from each navigator image using the sub-navigator as a reference. The matrix was then averaged along the row to obtain a single vector, containing the diaphragm position for each image acquisition. The concatenation of vectors from all navigator images exhibited a full respiration profile during the entire scan, shown in Figure 2c. The diaphragm position in each vector (red line in Figure 2c) was subsequently determined using an edge detection algorithm (17).

3. Control / label images selection. Final images were chosen during expiration. An acceptance window width of 8mm (2 pixel width in the navigator profile) was used. Control and label images of which diaphragm position was contained within the acceptance window were selected for the perfusion calculation. Note the final number of selected control and label images may differ from each other.

Images selected for the final perfusion calculation were realigned using the FMRIB's Linear Image Registration Tool (FLIRT, FMRIB, Oxford, United Kingdom) (18). The first image in the selected image series was used as the reference. The corrected images were then averaged to obtain a single control and label image. The perfusion weighted image was computed by subtracting the averaged control from the averaged label image.

Perfusion Quantification—Neglecting the transit effects and the exchange times between blood water molecule and the kidney tissue, the quantitative renal blood flow can be calculated pixel-by-pixel using a single compartment model (8)

$$f=\frac{\lambda}{2\alpha TI}\frac{\Delta M\,(TI)}{M_0}exp\left(\frac{TI}{T_1}\right)$$

where *f* is the perfusion rate (in the unit of ml/100g/min), λ is the blood-tissue water partition coefficient, which is assumed to be 80 ml/100g (19), α is the inversion efficiency which is assumed to be 0.95, $\Delta M(TI)$ is the perfusion weighted image, M_0 is the equilibrium magnetization of the tissue (proton density). The T_1 value of 1.15 sec for renal cortex (20) is assumed to be the T_1 of the blood. Pixels with exceptionally high perfusion values (f > 600 ml/100g/min) corresponding to macroscopic blood vessels (8) were all set to 600. In addition, perfusion values between 400 ml/100g/min and 600 ml/100g/min were set to 400 ml/100g/min according to the maximal possible value (8).

Image Analysis

Mean perfusion values were measured in renal cortex and medulla in both kidneys. Regions near renal arteries with extremely high perfusion values (*f* > 600 ml/100g/min) that correspond to macroscopic flow were carefully avoided in the ROIs. An illustration of the ROI outlines is shown in Figure 2d. SNR was calculated as

$SNR=\left(\overline{S}_{\mathrm{control}}-\overline{S}_{\mathrm{label}}\right)/\sigma_{\mathrm{noise}}$, where $\overline{S}_{\mathrm{control}}$ and $\overline{S}_{\mathrm{label}}$ were the mean signals in the renal cortex of the averaged control and label images, and σ_{noise} was the standard deviation of the noise in the subtraction image. The acquisition efficiency for the free-breathing scans was defined as (N_{contrl} + N_{label}) / N_{total}, where N_{contrl} and N_{label} were the number of navigator-selected control and label images, and N_{total} is the total number of images acquired. The acquisition efficiency for breath-hold scans was 0.67 since the first control/label pair was discarded in the perfusion averaging. The relative SNR (rSNR), defined as the product of the SNR and the acquisition efficiency, was also calculated.

To estimate the optimal scan time, the imaging data was resorted into sets of 10, 20, 30, 40 and 50 control / label pairs in the original acquisition order, corresponding to 1, 2, 3, 4 and 5 minutes of acquisition time. Each set then underwent the same retrospective signal averaging process as previously described. The acquisition efficiency for each individual set was calculated.

Pairwise rSNR difference among free-breathing and breath-hold scans was tested using a paired two-tail t-test. A nonparametric Friedman's test was used for comparing set acquisition efficiency. A P value less than 0.05 was considered to indicate significance.

RESULTS

Healthy Volunteer Experiment 1

The FAIR True-FISP sequence with the 2D navigator produced renal perfusion images of excellent quality in volunteers. An example of perfusion maps is illustrated in Figure 3. The

renal cortex and medulla can be clearly depicted. Subtraction errors and reduced SNR were apparent in the cortex in the breath-hold images (white arrow, Figure 3). Despite the longer readout duration, excellent image quality with improved delineation of cortex and medulla was obtained with the high resolution protocol (Figure 4). The realignment correction values are plotted in Figure 5a. The largest kidney motion after the retrospective selection was in the superior-inferior direction with a maximum displacement of 4 mm among all subjects. The average displacement was 1.1 mm along superior-inferior direction, and less than 1mm along the medial-lateral direction. In-plane rotation variation was less than 1 degree.

One volunteer had a solitary kidney and the result was excluded from the group analysis. The mean perfusion values measured in the healthy volunteers are reported in Table 1. The quantitative perfusion rate in the renal cortex ranged from 196 to 308 ml/100g/min with the coronal navigator, 219 to 328 ml/100g/min with the sagittal navigator and 182 to 368 ml/100g/min for the breath-hold scans. These values were in good agreement with other renal ASL studies in the literature (7,8,19,21). The perfusion rates measured in the solitary kidney was higher than the average (cortex: 364 ml/100g/min, medulla: 61 ml/100g/min), which was consistent with the known increase in size and function to compensate for the missing kidney (22,23).

The SNR, acquisition efficiency and rSNR for each healthy volunteer is reported in Table 2. The mean SNR was 36.65 for the coronal navigator, 31.36 for the sagittal navigator, and 12.15 for breath-hold scans. Overall, an average acquisition efficiency of 50 ± 13% and 41 ± 9% was observed for the coronal and sagittal 2D navigators, respectively. Acquisitions with the coronal navigator yielded slightly higher rSNR, however, there was no significant difference in rSNR between the coronal and sagittal navigator-gated acquisitions ($P > 0.05$). The rSNR of the free-breathing acquisitions using 2D navigator was significantly higher than the breath-hold acquisitions ($P < 0.05$).

An example of the retrospective reconstruction result for the multiple time sets is illustrated in Figure 6a. Figure 6b shows the mean SNR and acquisition efficiency across all healthy subjects. No significant difference was found ($P > 0.05$). The image quality gradually improved as the number of averages increased. The qualitative assessments of the image quality suggested the scan time might be reduced to 3 minutes and still maintain acceptable SNR (an average of 18) as the 5 minutes acquisition.

Healthy Volunteer Experiment 2

An example of varying imaging parameters including inversion slab thickness, imaging plane orientation, and respiratory pattern is illustrated in Figure 7. When the imaging orientation is oblique coronal, subtraction errors were highly apparent with the 10mm inversion band in both normal and deep breathing conditions. Imaging artifact was apparent with the 20mm inversion band during deep breathing. No apparent artifact was observed with the 30mm inversion band for both breathing patterns in the oblique coronal orientation.

The imaging result was much more prone to error in the axial imaging orientation. A reasonable perfusion renal image, judged by the cortico-medullary contrast, was only obtained with the 30 mm inversion band thickness and normal breathing in the axial imaging

orientation. The motion correction values are shown in Figure 5b. In general, the motion correction parameters had larger standard deviations for deep breathing in comparison with normal breathing.

Patient Experiment

The mean renal blood flow values in our patient study (n = 5) were 158 ± 27 and 151 ± 23 ml/100g/min for the left and right renal cortex; 34 ± 6 and 35 ± 6 ml/100g/min for the left and right renal medulla (Table 3). An average of 35 % acquisition efficiency was achieved in patients. No significant difference in acquisition efficiency between patients and healthy volunteers in experiment 1 was observed ($p > 0.05$). Compared with the health volunteers in experiment 1, both cortical and medullary perfusion rates were significantly lower in patients ($p < 0.01$). The perfusion map of a 58 year old male patient with stage 2 CKD is shown in Figure 8.

DISCUSSION

Like other abdominal MRI techniques, respiratory motion presents a major challenge in renal ASL studies. A variety of acquisition strategies have been proposed to overcome this problem. Breath-holding is commonly used to reduce respiratory motion, however, it still suffers from some degrees of residual motion (13) and often does not accommodate for sufficient signal averaging required by ASL. In addition, breath-holding can be difficult to tolerate for patients. Synchronized breathing or multiple breath-hold acquisitions (10) may offer sufficient signal averaging; however, it is impossible to guarantee the subjects to hold their breath at the exact position in the respiratory cycle. Those acquisition schemes usually requires additional patient training, and can be time consuming and impractical for routine clinical use. Respiratory triggering (13) can yield significantly different results based on the quality of the bellow waveform, which can vary from subject to subject depending on the position of the respiratory belt and the breathing pattern. Alternatively, prospective navigator echo gating technique such as the dual navigator echo (24) can be used to monitor kidney motion.

In our study, we demonstrated the feasibility of a novel 2D navigator to measure kidney perfusion with automated retrospective post-processing. The technique has effectively minimized the subtraction errors related to control and label image misalignment, and provided excellent image quality. Compared to the breath-hold technique, the 2D navigator-gated technique offered a near three-fold increase in SNR in healthy volunteers and drastically improved image quality in patients (it was difficult to assess the actual SNR improvement in patients since the actual perfusion signal in the cortical region in the breath-hold acquisitions was too low to be accurately measured using ROI analysis). The measured global renal perfusion was significantly lower in CKD patients than healthy volunteers. This finding is consistent with the recent literature (25), which suggested the importance of renal perfusion assessment as an indicator of compromised renal function. Our preliminary results have confirmed that ASL True-FISP can quantify kidney perfusion in the kidney in the CKD patients, given sufficient signal averaging. The 2D navigator provided a feasible method to accomplish this, whereas breath-hold did not.

The acquisition efficiency of the 2D navigator ranged from 35% - 65% depending on the respiratory pattern. Although the mean acquisition efficiency was higher in healthy volunteers than patients, the difference was not significant ($p > 0.05$). Larger sample size is required to understand whether a direct correlation between acquisition efficiency and the health state of the subject exists. In our experiments, the 5-minute imaging time was sufficient for all healthy volunteers, even with the high resolution protocol (which the nominal voxel size was reduced by 85%). Furthermore, our retrospective reconstruction with variable acquisition times suggested the scan time may be further reduced to 3 minutes without affecting the image quality.

Since the 2D navigator was implemented as an independent module, it could be combined with other ASL preparation (e.g. STAR(26), FAIR(11), PCASL(27)) and acquisition (e.g.True-FISP (8), EPI (13), SSFSE(10)) schemes. We chose the FAIR TrueFISP implementation for our ASL imaging due to the high inversion efficiency of the FAIR preparation and SNR advantage of the True-FISP readout (8). The central frequency was offset carefully from 0 – 50 Hz to avoid True FISP banding artifacts affecting the kidney. At 3T, the True-FISP catalyzation pulses with linearly increasing flip angles provided better suppression of transient signal oscillations compared to the $\alpha/2$ catalyzation pulse (data not shown).

The width of the acceptance window can impact the image quality and final acquisition efficiency. Too narrow of an acquisition window may result in insufficient SNR, and too wide of an acquisition window may lead to the inclusion of incorrect imaging slices rendering image artifacts. For illustration purpose, we reprocessed a deep-breathing case from experiment 2 with different acceptance window widths, as shown in Figure 9. The degradation of the image quality was clear as the acceptance window width increased. Subjects with smaller fluctuations of the diaphragmatic position during normal breathing may tolerate a wider acceptance window. In addition, imaging position can also affect the decision on the acceptance window width. Imaging in the axial or oblique coronal position, especially with a larger tilting angle would be more susceptible to subtraction errors with a wider acceptance window than imaging in the true coronal position. In our studies, because the imaging plane was in the oblique coronal position to best match the longitudinal axis of both kidneys for maximum coverage, we found an acceptance window of 8 mm was optimal for both volunteers and patients. Since the decision on the acceptance window width is a part of the post-processing, one may trade between SNR and image quality to determine the optimal acceptance window width for each individual case. .

The selective averaging algorithm for retrospective reconstruction was effective, easy to implement and computationally inexpensive. The sub-navigator position can be manually adjusted as needed. In our study, the algorithm to auto-identify the sub-navigator position provided satisfactory results for all case except one patient. In that particular case, the patient had a large liver such that the motion detected by the navigator did not correlate to the motion of the kidney. The sub-navigator was manually adjusted to gate off the spleen, and the perfusion map quality was greatly improved.

Our preliminary results showed the 2D navigator approach in its current implementation did not enable perfusion assessment in the axial imaging orientation when the subject exhibited a deep breathing pattern. Large motion along the superior-inferior direction can cause mismatch of the imaging slice leading to artifactual perfusion signal. Caution should be taken when imaging in the axial plane, especially when large fluctuations in the navigator profiles are observed. The 2D navigator approach worked well with the oblique coronal imaging position, even with a lower than recommended labeling inversion thickness. During the normal breathing exercise, we have observed the perfusion signal in the oblique coronal plane with the 20mm inversion thickness was slightly higher than the 30 mm inversion thickness across all three subjects. While we do not know the exact cause, it may be the result of a shorter inflow time due to the thinner inversion band. This observation will be investigated in future studies. Currently we recommend measuring renal perfusion with the 2D navigator technique applied in the coronal or oblique coronal orientation and using an inversion band at least 3.5 times thicker than the acquired slice thickness.

A few limitations of the study should be noted. Only retrospective navigator gating was used in this preliminary study due to the freedom of post-processing suitable for preliminary testing. Future implementations could include prospective gating which may aid more widespread utility. We are currently limited to single-slice imaging with the 2D navigator technique. Multi-slice imaging may be possible with parallel imaging of high acceleration factors and partial Fourier encoding without compromising scan time albeit at a cost of SNR and/or spatial resolution. Spatial variation in the transit delays of the labeled arterial spins, known as the transit time effect, was neglected in this preliminary feasibility study. While the use FOCI inversion pulses partially compensates for this effect (8), the final perfusion rates could be underestimated as a consequence. Alternatively, Q2TIPS (28) can be implemented to improve the accuracy of the perfusion quantification by employing additional saturation pulses. In our study, we only prescribed the 2D navigator in the coronal and sagittal plane since the kidney motion is predominately superior to inferior. Therefore, only in-plane rigid correction was applied. However, it is worth noting that imperfect in-plane motion correction can lead to misalignment between control and label images resulting in subtraction artifacts and inaccurate estimation of renal perfusion. Since conventional signal averaging in the presence of rotation and other nonrigid motion in the abdominal area would likely produce blurring, a more robust realignment method such as elastic model may be more appropriate.

Our experiments were carried out on a 3T scanner where the perfusion measurements benefited from an intrinsically higher SNR due to longer T1 values. The perfusion sensitivity can be further improved with background suppression (29) and PCASL labeling pulses (10,27). However, B1 inhomogeneity and off-resonance effects can compromise the labeling efficiencies of PCASL, especially in the abdomen. The specific absorption rate (SAR) may pose as another limitation for PCASL at 3T, although a recent study (9) has shown feasibility.

In summary, the 2D navigator gated ASL imaging was found to be a feasible method for quantifying renal perfusion without external contrast agent and compromising patient comfort. It provides a potential clinical solution for patients with impaired renal function

who may not tolerate breath-holding. In patients with reduced renal flow, perfusion sensitivity may be improved by increasing the number of signal averaging at a cost of increased scan time. A study with sufficiently large number of patients is warranted to test the effectiveness of this technique for routine clinical applications.

ACKNOWLEDGEMENT

This work is supported in part by NIH R21DK079080, R01DK093793 and AHA SDG0835367N. The authors thank Center for Advanced Imaging at NorthShore University HealthSystem for providing scan time and Drs. Wei Li and Ewa Gliwa for their technical and/or administrative assistance.

References

1. Huang AJ, Lee VS, Rusinek H. Functional renal MR imaging. Magn Reson Imaging Clin N Am. 2004; 12(3):469–486. vi. [PubMed: 15271366]
2. Grobner T. Gadolinium--a specific trigger for the development of nephrogenic fibrosing dermopathy and nephrogenic systemic fibrosis? Nephrol Dial Transplant. 2006; 21(4):1104–1108. [PubMed: 16431890]
3. Marckmann P, Skov L, Rossen K, Dupont A, Damholt MB, Heaf JG, Thomsen HS. Nephrogenic systemic fibrosis: suspected causative role of gadodiamide used for contrast-enhanced magnetic resonance imaging. J Am Soc Nephrol. 2006; 17(9):2359–2362. [PubMed: 16885403]
4. Calamante F, Thomas DL, Pell GS, Wiersma J, Turner R. Measuring cerebral blood flow using magnetic resonance imaging techniques. J Cereb Blood Flow Metab. 1999; 19(7):701–735. [PubMed: 10413026]
5. Pollock JM, Tan H, Kraft RA, Whitlow CT, Burdette JH, Maldjian JA. Arterial spin-labeled MR perfusion imaging: clinical applications. Magn Reson Imaging Clin N Am. 2009; 17(2):315–338. [PubMed: 19406361]
6. Artz NS, Sadowski EA, Wentland AL, Grist TM, Seo S, Djamali A, Fain SB. Arterial spin labeling MRI for assessment of perfusion in native and transplanted kidneys. Magn Reson Imaging. 2011; 29(1):74–82. [PubMed: 20850241]
7. Fenchel M, Martirosian P, Langanke J, Giersch J, Miller S, Stauder NI, Kramer U, Claussen CD, Schick F. Perfusion MR imaging with FAIR true FISP spin labeling in patients with and without renal artery stenosis: initial experience. Radiology. 2006; 238(3):1013–1021. [PubMed: 16439565]
8. Martirosian P, Klose U, Mader I, Schick F. FAIR true-FISP perfusion imaging of the kidneys. Magn Reson Med. 2004; 51(2):353–361. [PubMed: 14755661]
9. Wu WC, Su MY, Chang CC, Tseng WY, Liu KL. Renal perfusion 3-T MR imaging: a comparative study of arterial spin labeling and dynamic contrast-enhanced techniques. Radiology. 2011; 261(3): 845–853. [PubMed: 22095996]
10. Robson PM, Madhuranthakam AJ, Dai W, Pedrosa I, Rofsky NM, Alsop DC. Strategies for reducing respiratory motion artifacts in renal perfusion imaging with arterial spin labeling. Magn Reson Med. 2009; 61(6):1374–1387. [PubMed: 19319891]
11. Kim SG. Quantification of relative cerebral blood flow change by flow-sensitive alternating inversion recovery (FAIR) technique: application to functional mapping. Magn Reson Med. 1995; 34(3):293–301. [PubMed: 7500865]
12. Ordidge RJ, Wylezinska M, Hugg JW, Butterworth E, Franconi F. Frequency offset corrected inversion (FOCI) pulses for use in localized spectroscopy. Magn Reson Med. 1996; 36(4):562–566. [PubMed: 8892208]
13. Gardener AG, Francis ST. Multislice perfusion of the kidneys using parallel imaging: image acquisition and analysis strategies. Magn Reson Med. 2010; 63(6):1627–1636. [PubMed: 20512866]
14. Deshpande VS, Chung YC, Zhang Q, Shea SM, Li D. Reduction of transient signal oscillations in true-FISP using a linear flip angle series magnetization preparation. Magn Reson Med. 2003; 49(1):151–157. [PubMed: 12509831]

15. Griswold MA, Jakob PM, Heidemann RM, Nittka M, Jellus V, Wang J, Kiefer B, Haase A. Generalized autocalibrating partially parallel acquisitions (GRAPPA). Magn Reson Med. 2002; 47(6):1202–1210. [PubMed: 12111967]
16. Haralick, RM.; Shapiro, LG. Computer and Robot Vision. Addison-Wesley; 1992.
17. Canny J. A computational approach to edge detection. IEEE Trans Pattern Anal Mach Intell. 1986; 8(6):679–698. [PubMed: 21869365]
18. Jenkinson M, Bannister P, Brady M, Smith S. Improved optimization for the robust and accurate linear registration and motion correction of brain images. Neuroimage. 2002; 17(2):825–841. [PubMed: 12377157]
19. Karger N, Biederer J, Lusse S, Grimm J, Steffens J, Heller M, Gluer C. Quantitation of renal perfusion using arterial spin labeling with FAIR-UFLARE. Magn Reson Imaging. 2000; 18(6): 641–647. [PubMed: 10930773]
20. de Bazelaire CM, Duhamel GD, Rofsky NM, Alsop DC. MR imaging relaxation times of abdominal and pelvic tissues measured in vivo at 3.0 T: preliminary results. Radiology. 2004; 230(3):652–659. [PubMed: 14990831]
21. Roberts DA, Detre JA, Bolinger L, Insko EK, Lenkinski RE, Pentecost MJ, Leigh JS Jr. Renal perfusion in humans: MR imaging with spin tagging of arterial water. Radiology. 1995; 196(1): 281–286. [PubMed: 7784582]
22. Maluf NS. On the enlargement of the normal congenitally solitary kidney. Br J Urol. 1997; 79(6): 836–841. [PubMed: 9202546]
23. Maluf NS, Ford RV, Spurr CS. Physiology of the human solitary kidney. J Urol. 1957; 78(2):117–131. [PubMed: 13449999]
24. Song R, Loeffler RB, Hillenbrand CM. Improved renal perfusion measurement with a dual navigator-gated Q2TIPS fair technique. Magn Reson Med. 2010; 64(5):1352–1359. [PubMed: 20593428]
25. Rossi C, Artunc F, Martirosian P, Schlemmer HP, Schick F, Boss A. Histogram analysis of renal arterial spin labeling perfusion data reveals differences between volunteers and patients with mild chronic kidney disease. Invest Radiol. 2012; 47(8):490–496. [PubMed: 22766911]
26. Edelman RR, Siewert B, Darby DG, Thangaraj V, Nobre AC, Mesulam MM, Warach S. Qualitative mapping of cerebral blood flow and functional localization with echo-planar MR imaging and signal targeting with alternating radio frequency. Radiology. 1994; 192(2):513–520. [PubMed: 8029425]
27. Wu WC, Fernandez-Seara M, Detre JA, Wehrli FW, Wang J. A theoretical and experimental investigation of the tagging efficiency of pseudocontinuous arterial spin labeling. Magn Reson Med. 2007; 58(5):1020–1027. [PubMed: 17969096]
28. Luh WM, Wong EC, Bandettini PA, Hyde JS. QUIPSS II with thin-slice TI1 periodic saturation: a method for improving accuracy of quantitative perfusion imaging using pulsed arterial spin labeling. Magn Reson Med. 1999; 41(6):1246–1254. [PubMed: 10371458]
29. Ye FQ, Frank JA, Weinberger DR, McLaughlin AC. Noise reduction in 3D perfusion imaging by attenuating the static signal in arterial spin tagging (ASSIST). Magn Reson Med. 2000; 44(1):92–100. [PubMed: 10893526]

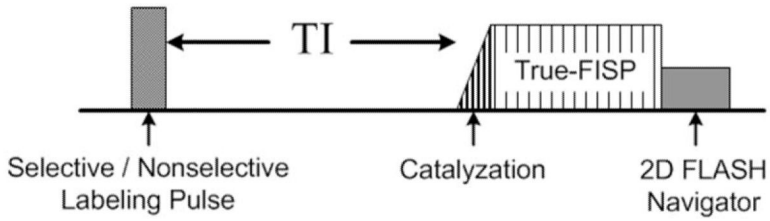

Figure 1.
Pulse sequence diagram for FAIR True-FISP with 2D FLASH navigator.

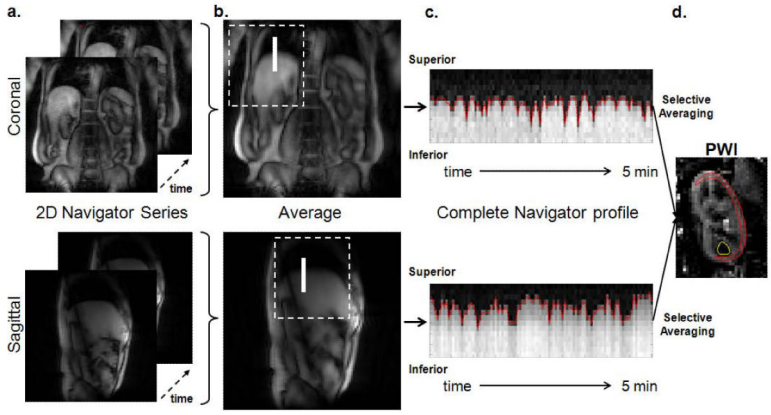

Figure 2.

The automated process of identifying the sub-navigator. (a) Examples of the 2D navigator images. (b) Averaged navigator images. The dotted square indicates the region extracted for the normalized 2D correlation calculation with the predefined template matrix. The resulting sub-navigator region is indicated by the white solid line. (c) The navigator profile across the entire acquisition. The red dotted line indicates the diaphragmatic position identified by the edge detection algorithm. (d) A perfusion weighted image (PWI) can be obtained by subtraction after selective averaging. An example of renal cortex and medulla ROIs are illustrated with red and yellow lines, respectively.

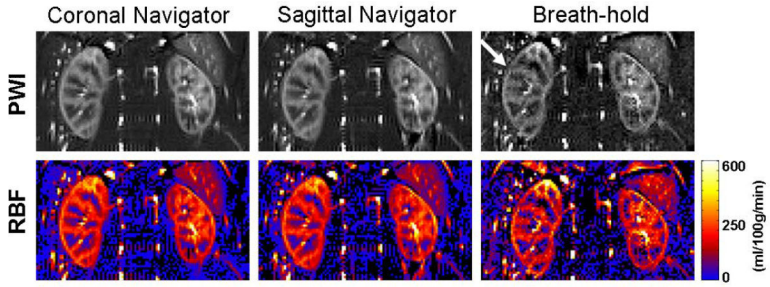

Figure 3.

Perfusion weighted images (PWI) and renal perfusion maps (RBF) obtained in a 49 year old healthy volunteer (subject 1 in table 2) using various acquisitions and averaging schemes.

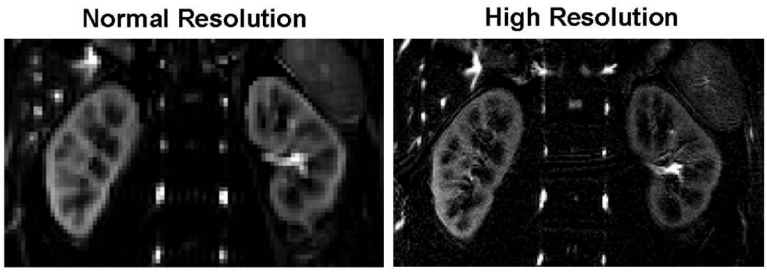

Figure 4.

A comparison between normal resolution ($3 \times 3 \times 8$ mm^3) and high resolution ($1.5 \times 1.5 \times 5$ mm^3) perfusion weighted image obtained from a healthy volunteer (subject 5 in Table 2).

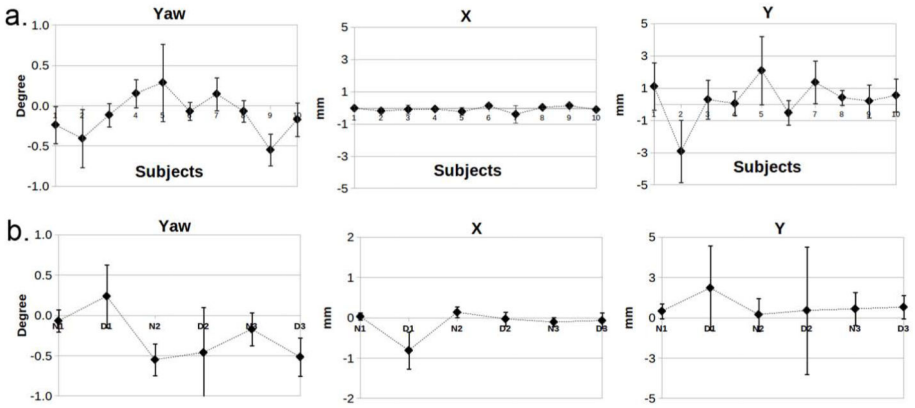

Figure 5.

Motion correction results from FSL FLIRT from experiment 1 (a) and 2 (b). The letter in the x-label for (b) indicates the breathing pattern: N – normal, and D – deep. The preceding numeral indicates the subject ID.

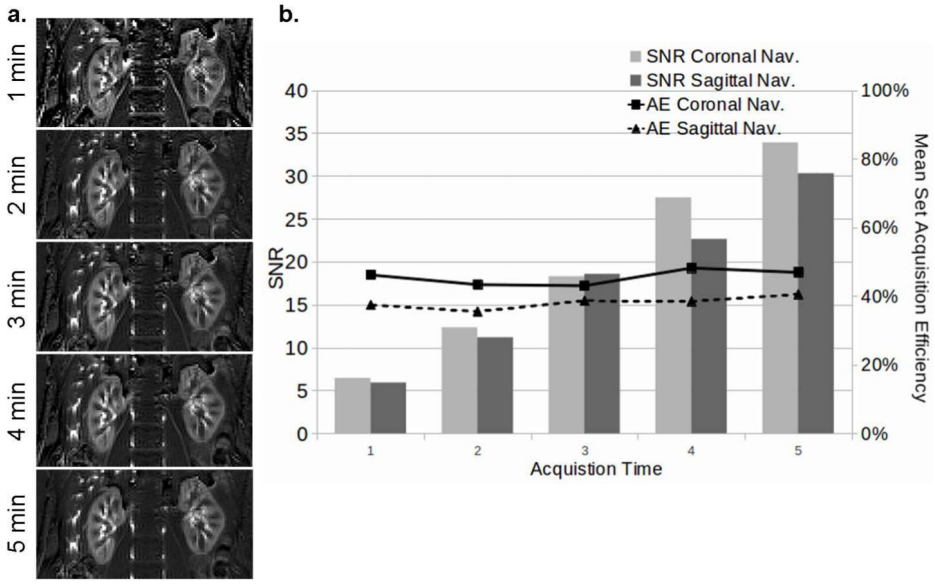

Figure 6.

Reconstruction results of multiple sets with variable acquisition lengths. (a) Perfusion weighted images retrospectively reconstructed from data acquired in an increment of 1 minute with 2D coronal navigator (subject 4 in Table 2). (b) A plot of mean SNR (bar chart) and set acquisition efficiencies (AE) (which remained relatively constant) versus acquisition time.

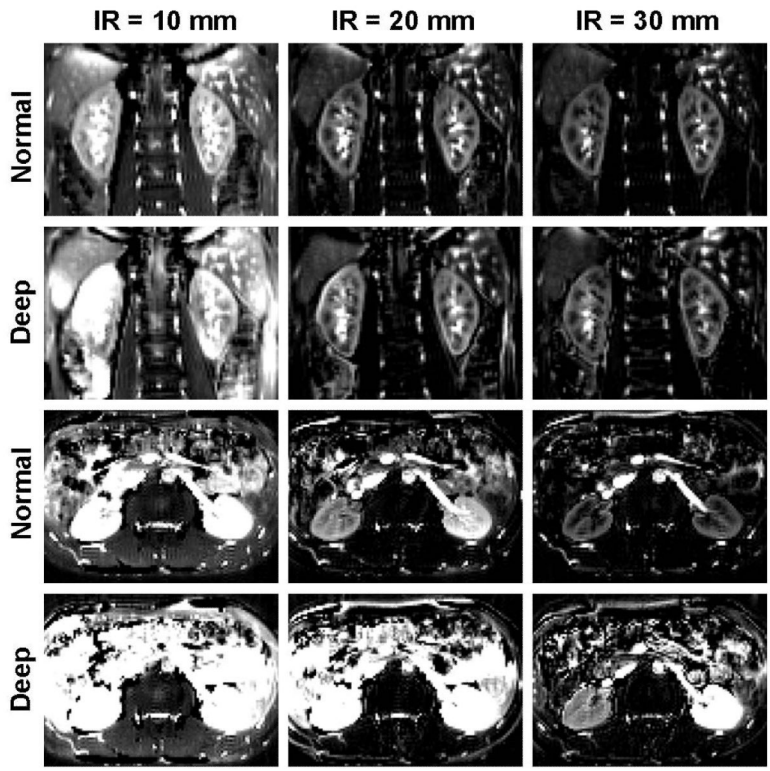

Figure 7.

Perfusion weighted images from a healthy volunteer (male, age of 25) with different imaging planes, labeling inversion band (IR) thicknesses and breathing patterns. Coronal acquisitions with 30 mm label thickness allowed for best perfusion images irrespective of the breathing pattern.

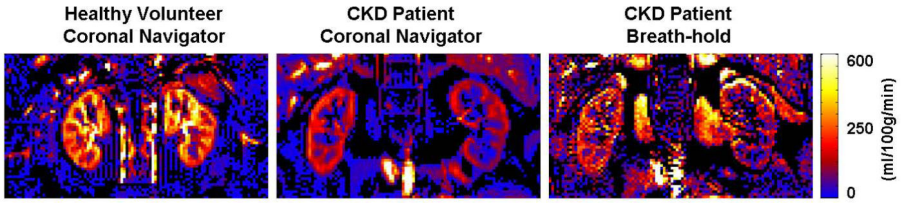

Figure 8.

The renal perfusion map from one of the patients (CKD stage 2, male, 58 years of age). Reduced global perfusion in the cortex was observed compared to a healthy volunteer (subject 6 in Table 2). The SNR and image quality of the breath-hold acquisition for the patient was too poor to be useful. The navigator-gated sequence allowed sufficient signal averaging to provide a reasonable perfusion map in the patient.

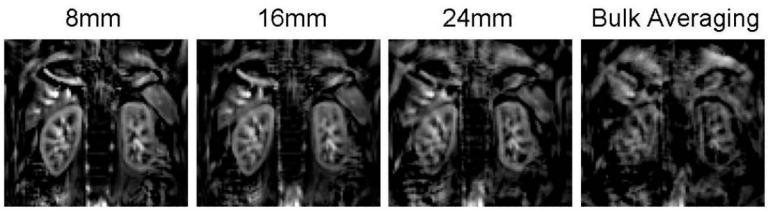

Figure 9.
Perfusion weighted image reconstructed with different acceptance window width.

Table 1

Mean perfusion rates (ml/100g/min) for healthy volunteers in experiment 1.

	Cortex		Medulla	
Acquisition Type	Left Kidney	Right Kidney	Left Kidney	Right Kidney
Coronal 2D navigator	274 ± 28	264 ± 25	65 ± 11	63 ± 15
Sagittal 2D navigator	278 ± 29	265 ± 34	59 ± 17	55 ± 18
Breath-hold	287 ± 38	281 ± 55	54 ± 11	48 ± 18

Table 2

SNR, acquisition efficiency and rSNR measurements of healthy volunteers.

	SNR			**Acquisition Efficiency ($N_{control}$, N_{label})**		**rSNR**		
Subj.	Coronal Nav	Sagittal Nav	Breath-hold	Coronal Nav	Sagittal Nav	Coronal Nav	Sagittal Nav	Breath-hold
1	29.53	27.24	6.98	65% (31, 34)	43% (22, 21)	19.20	11.71	4.61
2	38.91	31.32	12.45	61% (29, 32)	33% (16, 17)	23.74	10.34	8.22
3	23.54	20.05	9.71	37% (18, 19)	34% (15, 19)	8.71	6.82	6.41
4	28.67	29.24	14.02	35% (18, 17)	50% (24, 26)	10.03	14.62	9.25
5	46.02	39.49	13.19	54% (30, 24)	56% (32, 24)	24.85	22.12	8.71
6	47.28	27.90	13.06	58% (30, 28)	34% (16, 18)	27.42	9.49	8.62
7	23.39	19.02	8.22	38% (19, 19)	38% (17, 21)	8.89	7.23	5.43

Table 3

Perfusion rates (ml/100g/min) for CKD patients.

Patient	Cortex		Medulla		Acquisition Efficiency	Sex/Age	CKD Stage
	Left	Right	Left	Right			
1	160	158	36	31	38%	M / 83	4
2	149	161	40	45	39%	F / 57	3
3	170	177	34	36	32%	F / 67	4
4	119	116	36	35	26%	F / 54	4
5	191	147	24	29	39%	M / 58	2